JOURNAL OF BACTERIOLOGY, July 1975, p 7-19

Vol. 123, No. 1
Printed in U.S.A.

Control of Cell Length in *Bacillus subtilis*

MICHAEL G. SARGENT

National Institute for Medical Research, Mill Hill, London NW7 1AA, United Kingdom

Received for publication 24 March 1975

During inhibition of deoxyribonucleic acid synthesis in *Bacillus subtilis* 168 Thy⁻ Tryp⁻, the rate of length extension is constant. A nutritional shift-up during thymine starvation causes an acceleration in the linear rate of length extension. During a nutritional shift-up in the presence of thymine, the rate of length extension gradually increases, reaching a new steady state at about 50 min before the new steady-state rate of cell division is reached. The steady-state rates of nuclear division and length extension are reached at approximately the same time. The ratio of average cell length to numbers of nuclei per cell in exponential cultures is constant over a fourfold range of growth rates. These observations are consistent with: (i) surface growth zones which operate at a constant rate of length extension under any one growth condition, but which operate at an absolute rate proportional to the growth rate of the culture, (ii) a doubling in number of growth zones at nuclear segregation, and (iii) a requirement for deoxyribonucleic acid replication for the doubling in a number of sites.

The shape and dimensions of a bacterium must reflect the processes by which the external layers or shape-determining structures grow. Rod-shaped bacteria, such as *Bacillus*, probably grow only in length, as there is very little variation in width among cells of different age under any one growth condition (22). This could be achieved by large numbers of growth zones operating all over the surface or by a few annular zones. Studies of surface labeling of rod-shaped bacteria have provided evidence in favor of both views (11, 23–25, 32). The recent studies of Kepes and Autissier (14) in *Escherichia coli* have suggested that some membrane proteins may be the only surface components that exhibit conservation during growth and that lipid and mucopeptide are either randomized during growth or are inserted over the entire surface. In corroboration of this conclusion, Ryter et al. (33) have shown localized incorporation of diaminopimelic acid in very short pulses in *E. coli*. Probably the most satisfactory synthesis of the data available is that in rod-shaped organisms there are a limited number of growth zones but that certain components of the surface may appear not to be conserved, either because they are randomized after synthesis, or they are indeed synthesized all over the surface, or there is turnover of surface components.

The time course of length extension in rod-shaped organisms has been studied on individual growing cells (17), on populations of synchronous cells (41), and by inference from the length distribution of exponential-phase cultures (3). Such results show that length extension is undoubtedly continuous throughout the cell cycle but do not distinguish between exponential and linear growth models with certainty. Biochemical evidence that indirectly favors linear growth has been obtained by showing that mucopeptide in *E. coli* (10) and membrane protein in *Bacillus subtilis* (35) are synthesized at a constant rate with doublings in rate at particular points in each cycle. The pattern of synthesis of these components during the cell cycle might be expected to correspond with that of growth in length of the bacterium.

The suggestion of Jacob et al. (12) that chromosome segregation is achieved by surface growth between attached chromosomes imposes certain limitations on possible models of surface growth (36). An important conclusion from attempts to devise schemes of chromosome segregation depending solely on surface growth is that segregation can only be achieved with one or two growth zones per chromosome (36). The strongest support for the replicon hypothesis (12) remains the observation of Lark and co-workers (on *B. subtilis* [7], *E. coli* [21], and *Lactobacillus acidophilus* [1]) that labeled deoxyribonucleic acid (DNA) strands are not segregated randomly and that pulse-labeled chromosomes are inherited with the cell envelope to which it was attached when first used as a template. Pierucci and Zuchow-

ski (28) have confirmed these observations for *E. coli* and satisfactorily explained conflicting data. If chromosomes are segregated by surface growth, then temporal control of the appearance of surface growth zones should be coupled to chromosome replication (18, 29, 30, 43). In support of this, Kubitschek (18) has shown that volume increase in *E. coli* is linear in the absence of DNA synthesis, suggesting that the appearance of new growth zones is dependent on DNA replication.

There is strong evidence in *E. coli* that the chromosome cycle has a strict temporal relationship with cell separation (8). If the appearance of surface growth zones is coupled to a particular point in the chromosome cycle, then the length of a rod-shaped bacterium will be an exponential function of growth rate. Evidence for this has been obtained in a number of cases (37, 40, 43). Zaritsky and Pritchard (43) have suggested that the variation in average cell length with growth rate in *E. coli* is consistent with the appearance of growth zones at termination of replication and with the rate of extension per growth zone being proportional to growth rate. In this communication, three models are discussed for the control of cell length, which provides a reasonable fit to the observed variation in cell length with growth rate. Experiments have been devised that test the assumptions underlying the derivation of these models.

MATERIALS AND METHODS

Organism. *B. subtilis* 168/S, an asporogenic variant of 168 Thy$^-$ Tryp$^-$, able to grow on succinate as the sole carbon source, was maintained in a freeze-dried state. *B. subtilis* 168 Nil, a PBSX$^-$ mutant of 168 Thy$^-$ Tryp$^-$, was kindly supplied by D. Karamata and was maintained as spores.

Growth conditions. The basal medium (34) used contains phosphate buffer (7.1 g of disodium hydrogen phosphate and 1.3 g of potassium dihydrogen phosphate [anhydrous] per liter, pH 7.3), magnesium sulfate (0.25 mg/ml), ferrous sulfate ($\cdot 7H_2O$) (1 μg/ml), and manganese sulfate ($\cdot 4H_2O$) (0.1 μg/ml). Thymine (10 μg/ml unless otherwise stated) and tryptophan (5 μg/ml) were subsequently added aseptically to give the final concentrations shown. Carbon and nitrogen sources were added as shown in Table 1. The amino acid mixture shown contains L-arginine, L-alanine, L-glutamic acid, glycine, L-histidine, L-isoleucine, L-leucine, L-lysine, L-proline, L-serine, L-threonine, and L-valine. The final concentration of each amino acid was 100 μg/ml (in media 7 through 13). In media 4 and 5, proline and arginine were present at 4 mg/ml. In media 1 through 3, the concentration of ammonium sulfate was 2 mg/ml and that of carbon sources was 4 mg/ml.

Inocula were grown in medium 3 and subsequently subcultured into the media described below, with inocula chosen to give cultures in the exponential phase of growth after overnight incubation. Thus, all measurements by the criteria of a constant ratio of optical density at 540 nm (OD_{540}) to particle number and DNA to OD_{540} (data to be given separately) over at least three generations have been made on bacteria that have been grown in the exponential phase for more than 15 generations and were in balanced growth. All steady-state measurements shown in Table 1 were obtained after the overnight culture (still growing exponentially) was subcultured into fresh prewarmed media to give an OD of 0.02, and measurements were made on cultures having OD values between 0.1 and 1.0. All cultures were grown at 35 C with vigorous aeration.

Measurement of growth. The mass of bacteria per milliliter of culture was expressed as OD_{540}. The OD_{540} is proportional to dry weight over the range of 0 to 1.0 for a culture in balanced growth. For cultures grown on succinate, glucose and glucose plus casein hydrolysate, the dry weight per unit of OD_{540} = 200 μg. Although OD measurements represent a measure of cell volume, a constant ratio of OD to dry weight under a wide range of conditions has commonly been observed (16).

Coulter counting. Particle counting was as described previously (34). All references to cell number represent the number of Coulter units.

Length measurements. Cell length was measured by using a Watson image-splitting eyepiece on heat-fixed cells stained with 0.01% crystal violet. Average lengths obtained, with unstained cells under phase optics and stained cells under normal optics, did not differ significantly. Measurements were made on 40 to 50 cells of two preparations from each sample. The standard error of the mean for each set of measurements was usually less than 5% of the mean.

Septa. Septa were counted on heat-fixed preparations of bacteria stained with 0.01% crystal violet (34). At least 200 cells were counted on two preparations of each sample. The frequency of septa (S) was expressed as a fraction of cells counted. The time elapsing between appearance of septa and cell separation is given by $(S + 1) = 2^{St}/g$, where St is the separation time and g is the generation time (see Appendix).

Nuclear staining. Heat-fixed specimens were hydrolyzed with 1 N HCl for 7 min at 60 C, washed in phosphate buffer (0.1 M, pH 7.3), stained with freshly prepared Giemsa stain (B.D.H.) (diluted 1:10 with phosphate buffer [0.1 M, pH 7.3] and filtered) for 5 min, and examined while they were still immersed in the stain. The nuclei in 200 cells in two preparations of each sample were counted and expressed as a fraction of the cells counted (i.e., Nu). The time elapsing between nuclear division and cell separation is given by $(Nu) = 2^{y}/g$, where y is time elapsing between nuclear division and cell separation (see below).

RESULTS

Models for length growth. The length of a rod-shaped organism that grows only in length

is determined by: (i) the number of growth zones, (ii) the rate of length extension per growth zone, and (iii) the time in each cycle over which length extension occurs. Expressions for the average length of cells in an exponential-phase population of bacteria have been derived by using the age distribution theorem (31), assuming either linear or exponential growth in length during the cell cycle (see Appendix). In each of the three models considered, the rate of length extension has been considered independently of the cell width. Models based on the rate of increase in surface area can be derived (30). However, in the case of the strain of *B. subtilis* used for the experimental tests described below, there is no detectable variation in cell width with growth rate. Therefore, any conclusions pertaining to cell length extension apply equally to surface area increase.

Linear growth models. Linear growth would occur during a period in which the number of growth zones did not change and the rate of length extension per site remained constant. Thus, in the cell cycle, if the number of growth zones doubled at time t (Fig. 1a) and the rate of length extension per site was constant, then the length of the cell would increase linearly with a doubling in rate at t. Two alternative models of linear growth have been considered.

(i) Model A. The rate of linear extension per site is constant at all growth rates. The average length ($\bar{L}$) is given by:

$$\bar{L} = (nl'/\log_e 2)\, g\, 2^{x/g}$$

where l' is a constant with dimensions of length per minute, x is the time elapsing between the doubling in number of growth zones and cell separation, g is generation time in minutes, and n is the number of growth zones present in a cell before the doubling in rate (i.e., cell age interval $0 - t$, Fig. 1A) when $x < g$.

(ii) Model B. The rate of length extension per site is proportional to growth rate, i.e.,

$$\bar{L} = (nl/\log_e 2)\, 2^{x/g}$$

where l is a constant with dimensions of length.

Exponential growth model. (iii) Model C. The number of sites increase exponentially, but the rate of length extension per site is constant under any one growth condition and varies in proportion to growth rate, i.e., $\bar{L} = nl\ 2^{x/g}$, where l is a constant with dimensions of length and n is the number of sites of length extension at x minutes before cell separation. This model is formally indistinguishable from model B, although the constants in each formula differ in significance. A number of alternative models have been considered (see Appendix). As with linear models, the relationship between the rate of extension per site and growth rate has the biggest effect on the form of the equation. The symbols l' and l have been used to distinguish constants with different dimension.

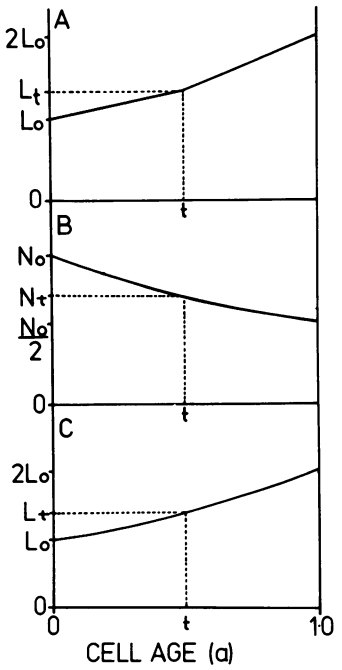

FIG. 1. *Relationship between cell length, relative cell age, and age distribution. (A) Linear growth in length with doubling in rate at relative cell age (t). (B) Age distribution given by* $N_{(a)} = No\ 2^{-a}$ *(31). (C) Exponential growth in length. Length at t (Lt) = Lo* 2^t. *Vertical axis is on arithmetic scale.*

Calculation of nuclear segregation time, septal separation time, and time of commitment to division. If an event occurs at a specific cell age in the cell cycle (i.e., t, Fig. 1B), the proportion of cells (p) in the population that have passed this point can be calculated from the age distribution theorem (31) by the formula $p = 2^{(1-t)}$ (where t is expressed in fractions of a generation time). Proofs of this relationship have been given by others (13, 20, 27).

The nuclear segragation time, septal separation time, and time of commitment to division can be determined by using this relationship as follows.

(i) The time elapsing between nuclear division and cell separation (y) is given by $Nu = 2^{y/g}$, where Nu is the average number of nuclei per cell. Note, y is expressed in real time.

(ii) The time between appearance of septa and cell separation (St) is given by $(1 + S) =$

$2^{St}/g$, where S is the average number of septa per growth unit and $(1 + S)$ is the average number of cells separated by a septum (i.e., if there is an average 0.1 septum per cell, the average number of separate cells is 1.1 per Coulter unit).

(iii) When DNA synthesis is inhibited (i.e., by thymine starvation in a thymine-requiring strain), only those cells that have completed their chromosomes are able to divide (4). The time elapsing between commitment to division (z) and cell separation is given by $Nd = 2^z/g \times 100$, where Nd is the percent increase in cell number over those present at zero time during thymine starvation. The time of commitment to division is defined as that time in the cell cycle at which cells proceed to division in the absence of DNA synthesis.

Effect of growth conditions on length, nucleation, and septation. The variation in average length, number of nuclei, and number of septa in *B. subtilis* 168/S grown under a wide variety of conditions is shown in Table 1. If ammonium sulfate is the sole nitrogen source and the carbon source is varied, growth rates between 0.5 and 1.0 generations per h are obtained. Arginine, proline, and glutamate will act as the sole carbon and nitrogen sources within the range of growth rates. Mixtures of amino acids in the presence of glucose allow growth rates of up to 2 generations per h.

The figures shown represent the average of at least two estimates of the parameters shown, made with bacteria from cultures in which growth rate and cell mass were very similar, if not identical. Many other experiments with these media have indicated that the growth rates are typical of the media, although large variations in generation time (120 to 105 min) were encountered with different batches of succinate-containing media.

All calculations have been based on numbers of particles per milliliter of culture (measured by a Coulter counter), since this is operationally convenient, although septum formation occurs substantially before cell separation.

Septa. The time elapsing between the appearance of the septum and cell separation can be calculated from the average number of septa per cell (Table 1). The average number of septa varies between 0.1 per average cell in slow-growing cells and 0.6 per cell in fast-growing cells. The calculated separation time is about 20 min under most conditions but is marginally longer in media 7 and 8. A separation time of 138 min (which is unaffected by growth rate) has been demonstrated in another strain of *B. subtilis* (27) under slightly different growth conditions. I have also shown that separation time can be varied by alteration in the ionic composition of the growth medium (34).

Nuclei. The appearance of Giemsa-stained

TABLE 1. *Nuclei, septa, and cell length in B. subtilis in relation to growth rate*

Medium[a]	Growth rate (divisions/h)	Nuclei/cell (Nu)	Segregation time[b] (y, min)	Septa/cell (S)	Septum separation time[c] (St, min)	Cell length ($\bar{L}$, μm)	$\bar{L}/Nu$
1	0.53	1.37	52	0.12	20	2.46	1.94
2	0.87	1.71	53	0.20	19	2.9	1.7
3	1.03	1.8	49	0.24	18	3.46	1.92
4	0.62	1.72	76	0.18	23	2.95	1.71
5	0.88	1.87	63	0.24	21	3.38	1.81
6	1.2	3.15	81	0.27	17	5.69	1.8
7	1.09	3.0	87	0.38	26	5.43	1.82
8	1.18	2.8	76	0.58	29	5.02	1.79
9	1.5	3.08	65	0.47	18	5.52	1.78
10	1.54	3.07	63	0.4	19	5.53	1.81
11	1.88	3.53	58	0.58	21	6.52	1.84
12	1.91	3.4	55	0.45	17	6.12	1.8
13	2.0	3.25	51	0.52	18	5.8	1.78
14	2.18	3.3	47	0.58	18	5.35	1.62

[a] Media: (1) Succinate-ammonia, (2) glycerol-ammonia, (3) glucose-ammonia, (4) proline, (5) arginine, (6) glucose-arginine, (7) glucose-amino acid mix minus valine, (8) glucose-amino acid mix minus methionine, (9) glucose-amino acid mix minus glutamate, (10) glucose-amino acid mix minus proline, (11) glucose-amino acid mix minus histidine, (12) glucose-amino acid mix minus lysine, (13) glucose plus complete amino acid mix, (14) glucose plus casein hydrolysate.

[b] Segregation time (y) calculated from $Nu = 2^y/g$.

[c] Septum separation time calculated from $(1 + S) = 2^{St}/g$.

nuclei in heat-fixed preparations is shown in Fig. 2. Nuclei are seen either in the center of cells or at 25% from either end (36) and can, therefore, be scored quite unambiguously since there are very few intermediate forms. Formalin-fixed nuclei, on the other hand, may appear as lobed structures and, in some preparations at high growth rates, these appear as separate nuclei, with the result that larger numbers of nuclei per cell are recorded. Neither image can be regarded as corresponding to the nuclear form in living bacteria, but there is evidence that nuclear division, as scored operationally with heat-fixed preparations, occurs at or close to the time of commitment to division (see Fig. 4a). Table 1 shows the number of nuclei per cell and the time between nuclear division and cell separation (y) as calculated above. Under most conditions, values for y of 45 to 65 min were obtained, although with organic nitrogen sources at lower growth rates the values of y were 60% longer than this.

Cell length. Each of the formulas for the theoretical models discussed above can be rearranged to give straight-line relationships of the form $a = mb + c$, as shown in Table 2 [models A through C (i)]. In each case, $\log_2 \bar{L}$ or $\log_2 \bar{L}/g$ is proportional to divisions per hour, and the slopes of the lines would then have values of x. The variation in average cell length with growth rate is shown in Fig. 3a and b, plotted as (a) $\log_2 \bar{L}/g$ and (b) $\log_2 \bar{L}$ against generations per hour. Both plots provide moderately good fits to a straight line (determined by least-squares regression analysis). However, in Fig. 3a x has a value of 118 ± 12 min and in Fig. 3b it has a value of 46 ± 10 min (Table 2).

The variation from a straight line seen in Fig. 3 indicates that x cannot be constant under all the growth conditions. This is probably accounted for by the variation in the time between nuclear division and cell separation (y) (Table 1), which would therefore alter x. The equations for each model can be modified to take this into

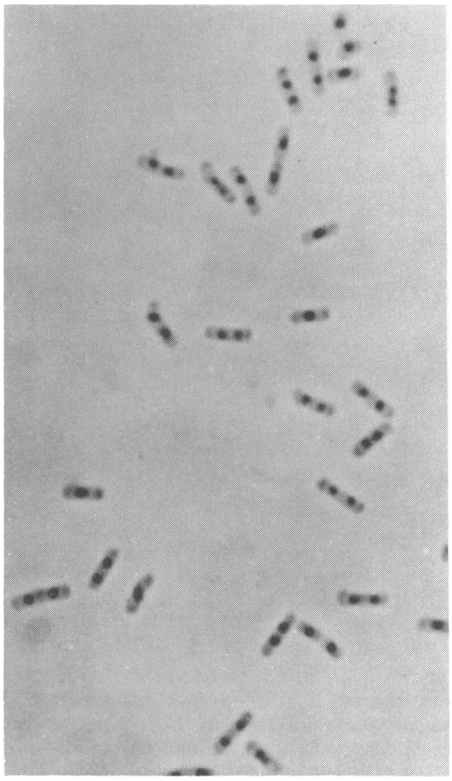

FIG. 2. *Giemsa-stained nuclei of B. subtilis 168/S grown in glucose-ammonium medium no. 3.*

TABLE 2. *Graphical analysis of three models of cell length extension.*

Model	Formula	Rearrangement[a]	$x \pm$ SE[a,b] or $(x - y)$ (min)	Best fit for intercept	Constant C[a]
A (i)	$\bar{L} = gnl'/\log_e 2 \cdot 2^x/g$	$\text{Log}_2(\bar{L}/g) = x\,(1)/(g) + \log_2(nl'/\log_e 2)$	118 ± 12.5	$\log_2(1.55 \times 10^{-2})$	$nl' = 1.07 \times 10^{-2}$ μm/min
B (i)	$\bar{L} = nl/\log_e 2 \cdot 2^x/g$	$\text{Log}_2\bar{L} = x\,(1)/(g) + \log_2(nl/\log_e 2)$	46 ± 10	$\log_2(2.3)$	$nl = 1.59\,\mu$m
C (i)	$\bar{L} = nl \cdot 2^x/g$	$\text{Log}_2\bar{L} = x\,(1)/(g) + \log_2 nl$	46 ± 10	$\log_2(2.3)$	$nl = 2.3\,\mu$m
A (ii)	$\bar{L}/Nu = gnl'/\log_e 2 \cdot 2^{x-y}/g$	$\text{Log}_2(\bar{L}/gNu) = (x - y)\,(1)/(g) + \log_2(nl'/\log_e 2)$	67 ± 5	$\log_2(1.93 \times 10^{-2})$	$nl' = 1.33 \times 10^{-2}$ μm/min
B (ii)	$\bar{L}/Nu = nl/\log_e 2 \cdot 2^{x-y}/g$	$\text{Log}_2(\bar{L}/Nu) = (x - y)\,(1)/(g) + \log_2(nl/\log_e 2)$	−3 ± 2	$\log_2(1.875)$	$nl = 1.29\,\mu$m
C (ii)	$\bar{L}/Nu = nl \cdot 2^{x-y}/g$	$\text{Log}_2(\bar{L}/Nu) = (x - y)\,(1)/(g) + \log_2 nl$	−3 ± 2	$\log_2(1.875)$	$nl = 1.875\,\mu$m

[a] Formula rearranged to form $a = mb + C$. Left-hand side = a; $m = x$ for models A (i), B (i), and C (i); $m = (x - y)$ for models A (ii), B (ii), and C (ii); b = $1/g$; and second term on the right = C.

[b] Standard error (SE) of regression coefficient.

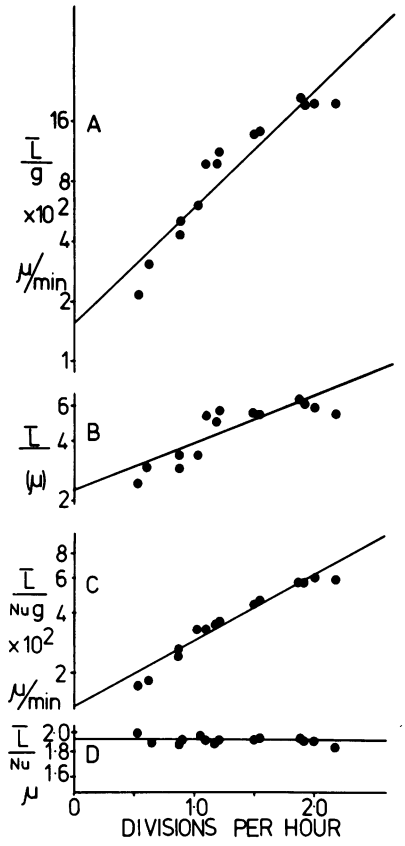

FIG. 3. *Relationship between cell length and growth rate. (A) $Log_2 \bar{L}/g$ plotted against growth rate (divisions per hour), where $\bar{L}$ is the cell length (micrometers). (B) $Log_2 \bar{L}$ plotted against growth rate. (C) $Log_2 \bar{L}/Nug$ plotted against growth rate. (D) $Log_2 \bar{L}/Nu$ plotted against growth rate.*

account by dividing each equation by that for the numbers of nuclei, i.e., $Nu = 2^y/g$. These relationships are shown in Table 2, together with the transformations for graphical analysis [models A through C (ii)]. Figure 3c and d shows $\log_2 \bar{L}/gNu$ or $\log_2 \bar{L}/Nu$ plotted against generations per hour. Model A gives a value of $(x - y)$ (the slope) of 67 ± 5 min, whereas modesl B and C give values of -3 ± 2 min. The latter is not significantly different from zero by Student's t test. In both cases, the fit to a straight line is substantially better than when plotted as in Fig. 3a and b. The fit to models B and C (Fig. 3d) is probably marginally better than for A. Thus, on the basis of model A, growth zones double in number 67 min before nuclear segregation, but, according to models B or C, x is reached at or close to nuclear segregation.

Effect of thymine starvation on length extension and cell division. In deriving the models of length extension suggested above, a specific temporal relationship between the time at which growth zones double in number and the time of cell separation has been proposed. The most tangible physical basis for such a relationship is that certain parts of the chromosome have to be replicated to generate new sites of length extension. If so, then during inhibition of DNA synthesis the rate of extension should remain constant at the rate determined by the number of preexisting sites. For an exponential culture, the rate of length extension at any length ($\bar{L}$) is $\bar{L}/g$. $Log_e 2$ and would be equal to the initial rate of extension on any model of growth. The constant-rate model A suggests that in a nutritional shift-up during thymine starvation the rate of length extension will remain unchanged, whereas model B suggests there should be an increased rate of length extension. DNA synthesis was inhibited by thymine starvation of strain Nil of *B. subtilis* 168, which lacks the defective phage PBSX and therefore does not lyse during this treatment. Also, Nil differs from 168/S (but is similar to 168 Thy^- $Tryp^-$) in that it grows more slowly in glucose minimal medium and has slightly larger cells (20% greater than 168/S). The average cell length per nucleus was not significantly different for the two strains. Prior to thymine starvation, the strain was grown on glucose-ammonium medium (3) (Table 2) with a generation time of 76 min and was then collected on a membrane filter (Millipore Corp.), washed free of thymine, and suspended in medium lacking thymine. Half of the resuspended culture was transferred to a flask containing casein hydrolysate to give a final concentration of 0.5%. During thymine starvation, the OD_{540} continued to increase exponentially for 2 h and then slowed quite markedly, finally giving a 2.5-fold increase over the initial value (Fig. 4a). Cell numbers increased to 160% (Fig. 4a), and then no further cell division occurred. At this stage, 20% of these cells contained septa so that the total increment in cells that formed septa over the initial concentration of cells (Coulter units) was 192%, which was reproducible to within 10%, although the proportion of septate cells remaining was lower in some experiments. Under these conditions, production of anucleate cells has not been seen (6). The point of commitment at which completely separate bacterial units are produced is, therefore, 54 min before cell separation, and that to produce a septum is about 70 min before cell separation

(calculated as shown above). The nuclear segregation time in this strain is also 70 min; therefore, commitment to septum formation occurs almost simultaneously with nuclear segregation.

The average length changes very little for 80 min after starvation but, thereafter, starts to increase considerably as the division rate falls (Fig. 4b). The rate of length extension can be considered independently of cell numbers by following the sum of cell lengths (i.e., average cell length $\times$ cell number). This is approximately linear for 4 h and gives a total increase of 2.5-fold (Fig. 4c).

A nutritional shift-up during thymine starvation has very little effect on the extent or rate of residual cell division (Fig. 4a). The mass growth rate is initially marginally higher and ultimately increases threefold before stopping. Cell length increases rapidly and, when plotted as the sum of cell lengths, is approximately linear for 4 h with a 4.5-fold increase in total length (Fig. 4c).

The rate of length extension with glucose as carbon source was 0.77×10^8 μm/h and during the shift-up was 1.72×10^8 μm/h. This is clearly not consistent with constant-rate model A. The rate of length extension predicted by model B can be calculated as follows:

rate of length extension per cell

$$= nl/g \times 2^{x}/g \times 60\,\mu\text{m/h}$$

The value of $2^x/g$ was shown above to be equal to the number of nuclei per cell, and a value of nl of 1.29 μm was obtained from length per nucleus (Table 2). For strain Nil grown on glucose the generation time was 76 min. The expected rate of extension per cell was therefore 0.8 μm/h and for 1.25×10^8 cells per ml would be 1.0×10^8 μm/ml of culture. The observed value was about 20% lower than this.

The typical postshift mass doubling time of exponential-phase cells for Nil was 40 min. During thymine starvation, the mass growth rate apparently did not reach this rate during a shift-up. However, the theoretical rate of length extension, calculated as above, using 40 min as a value of g, was 1.88×10^8 μm/h, and the observed rate was 10% lower than this.

Length extension during a nutritional shift in unstarved exponential-phase cells. When exponentially growing cells are shifted-up nutritionally, the mass growth rate accelerates to a new rate almost immediately (15, 37), whereas other processes, such as cell division or DNA synthesis, show a lag before reaching the new rate. For each process the time elapsing between the shift and attainment of the new steady state is equal to the length of time required from initiation of the process to completion (e.g., a new rate of chromosome initiation is reached $C + D$ minutes before cell division, where C is the chromosomal replication time and D is the time elapsing between termination and cell division) (8).

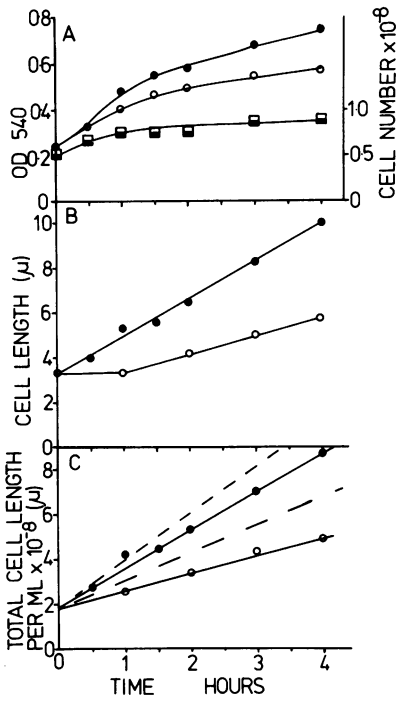

FIG. 4. *Effect of nutritional shift on growth in cell length during thymine starvation of B. subtilis Nil. Nil was grown on glucose-ammonium medium no. 3, collected on a Millipore filter, and washed with fresh medium lacking thymine. This was divided into two portions. Casein hydrolysate was added to one of these (final concentration 0.5%). (A) ○ and ●, OD_{540} for glucose and glucose plus casein hydrolysate, respectively; □ and ■, cell number per milliliter (Coulters units) for glucose and glucose plus casein hydrolysate. (B) ○ and ●, Cell length (micrometer) for glucose and glucose plus casein hydrolysate. (C) ○ and ●, Total cell length (i.e., cell number $\times$ average cell lenth) for glucose and glucose plus casein hydrolysate. (——) and (---) Theoretical rates for glucose and glucose plus casein hydrolysate, respectively.*

This priciple can be used to distinguish between model A and the other two. For the data shown above (Fig. 3, Table 2) to fit model A, the doubling in rate must occur approximately 70 min before nuclear segregation. In the transition from succinate to glucose (Table 1), this is about 120 min before the rate of cell division reaches a steady state. On the basis of

model B, x is equal to the time elapsing between nuclear segregation and cell division, which in the case of glucose-grown cells will be about 50 min before cell separation. In a nutritional transition, therefore, length extension should reach a steady state only 50 min before cell division. Clear-cut evidence against model A has been obtained in the transition from succinate to glucose medium.

Bacteria growing on succinate with a doubling time of 115 min were diluted with fresh, prewarmed medium containing 0.4% glucose. The mass growth rate accelerated almost instantaneously to a doubling time of 60 min, whereas cell numbers increased only gradually, reaching a new steady state after about 130 min (Fig. 5b). Figure 5a shows cell mass (OD per 10^9 cells), plotted on an arithmetic scale, together with cell length and numbers of nuclei during the transition. The latter two parameters changed most sharply in the interval 80 to 120 min. This could be explained as follows. If any event is controlled by a specific part of the chromosome, the product (on a per cell basis) will increase during the interval between this element reaching a new steady state of replication and the time at which the new steady state of cell division is reached. The sharp changes in numbers of nuclei and cell length between 80 and 120 min represent the time between the doubling in rate of length extension and cell division. The time of the transition can be seen more clearly, in this case, by plotting the time courses of total length increase and increase in numbers of nuclei per milliliter (Fig. 5b). Both nuclei and cell length reach steady states at about 80 min and not immediately after the shift-up. Model A is therefore most unlikely on this analysis.

The effect of the variable rate element on the time course of the transition is shown in Fig. 6, where the data for total length per milliliter of culture is shown, plotted on an arithmetic scale, relative to the theoretical initial rates of length extension calculated for values of g of 60 and 120 min. The initial rate of length extension falls about the rate to be expected for a culture with a generation time of 60 min, but over the first hour the difference between this and the rate for a generation time of 120 min is small and barely significant statistically. However, the overall trend appears consistent with model B.

DISCUSSION

The time taken to reach a new steady state of total length extension during a nutritional shift (from succinate to glucose) provides a critical

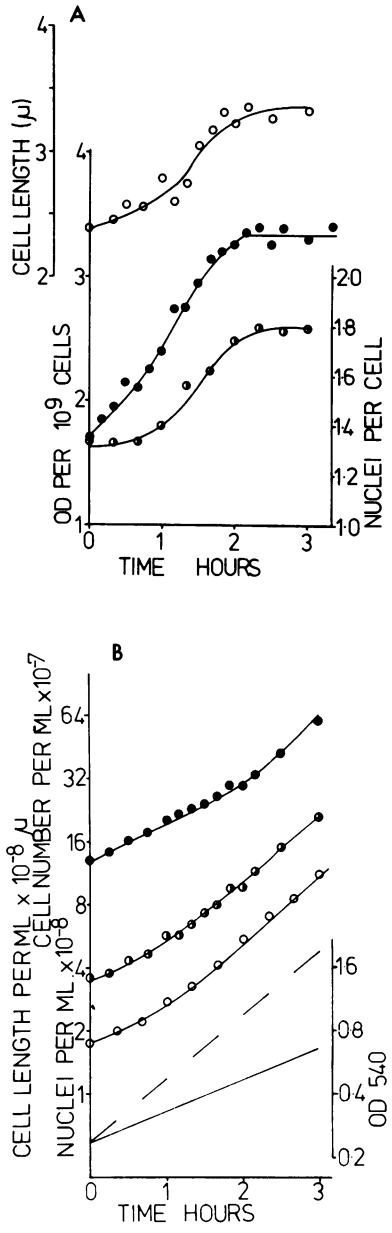

FIG. 5. *Effect of nutritional shift up on cell length and nucleation in B. subtilis 168/S. At zero time, glucose was added (final concentration 4 mg/ml) to an exponential-phase culture of B. subtilis 168/S growing on succinate-ammonium medium no. 1. Culture was diluted 1:1 with fresh medium after 90 min. All concentration figures after the dilution were multiplied by 2. (A) O, Average cell length (micrometers); ●, average cell mass, i.e., OD_{540} per 10^9 Coulter units; ◑, average number of nuclei per cell. All figures plotted on an arithmetic scale. (B) ●, Cell number (Coulter units) per milliliter; ◑, total cell length per ml, i.e., cell number × average cell length; O, total*

difference between models A and B. The new rate is reached after about 80 min, as predicted by model B, whereas model A predicts that a new rate would be reached soon after the transition. Sud and Schaecter (40) have also observed a lag in the rate of increase in total length during nutritional transition experiments in *Bacillus megaterium*.

A second difference between models A and B is that the rate of length extension per site is constant at all growth rates in the former case and variable in the latter. Strong support for the variable-rate model (B) has been obtained by demonstrating an acceleration in rate of length extension during a nutritional shift-up of bacteria starved of thymine. This experiment is based on the assumption that inhibition of DNA synthesis (by thymine starvation) prevents the appearance of new sites of length extension but allows length extension from preexisting sites and, indeed, during thymine starvation the rate of total length extension is linear, both during a nutritional shift-up and in unshifted cultures. Kubitschek (18), using *E. coli*, has shown a linear increase in volume over two generations during thymine starvation.

Although exponential models cannot be eliminated by this analysis, a small amount of indirect evidence against them is available. Thus, synthesis of mucopeptide in *E. coli* (10) and membrane protein in *B. subtilis* (35) occur linearly with doublings in rate at specific times in each cycle, and these might be expected to correspond to the pattern of length growth shown by the organism. If there are indeed small numbers of growth zones (11, 14, 32, 33) in rod-shaped bacteria, to sustain linear growth each site would have to extend at an exponentially increasing rate. The thymine starvation experiments suggest this is unlikely.

On the basis of either model B or C, the cell length at nuclear division is a constant or multiple thereof at all growth rates (see Appendix) and, furthermore, nuclear segregation in 168/S occurs in cells of the same range of lengths (2.5 to 3.0 μm) in both succinate- and glucose-grown bacteria in which the average cell lengths are 2.4 and 3.5 μm, respectively (36). Nuclei in mononucleate cells are found in the center of cells, and at nuclear division the daughter nuclei appear to move abruptly to a site 25% from either end of the cell (36). Thus,

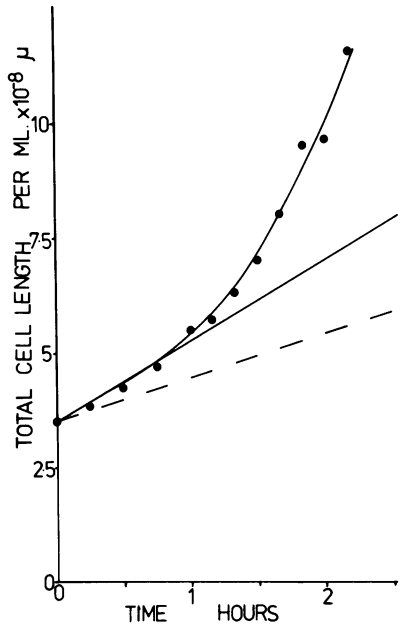

FIG. 6. *Comparison of rate of length extension with theoretical rates during shift-up.* (●) *Total cell length per milliliter (cell length × cell number per milliliter) plotted on arithmetic scale. Data from Fig. 5B.* (---) *Theoretical rate of length extension at zero time for preshift culture grown at generation time of 120 min.* (——) *Theoretical rate of length extension at zero time for culture grown at generation time of 60 min.*

during nuclear division the distance moved by nuclei on either side of the center is the same at all growth rates.

If, as Jacob et al. (12) have suggested, chromosome segregation is achieved only by surface growth between attached chromosomes, there can be only one or two growth zones per chromosome (36). Thus, either there is one growth zone, generating surface symmetrically on either side (36), or there are two asymmetric growth zones flanking the newly synthesized part of the surface (as suggested by Donachie and Begg [5]). Ryter and colleagues (32, 33) have provided evidence for symmetrical growth zones in *B. subtilis* and *E. coli*.

The apparent "jump" in the position of the nuclei appears superficially to be incompatible (36) with the idea that surface growth between chromosomal attachment sites achieves segregation (12). However, this observation can be reconciled with the theory as shown in Fig. 7. The chromosome is shown attached to the cell surface by the terminus at a growth zone (symmetrical) and at the next potential growth zone by the origin, with the bulk of the nucleus located at the terminus attachment site. As

number of nuclei per milliliter (cell number per ml × average number of nuclei per cell). (---) OD_{540} *in post-shift culture.* (——) *Preshift growth rate* (OD_{540}). *All figures plotted on log scale.*

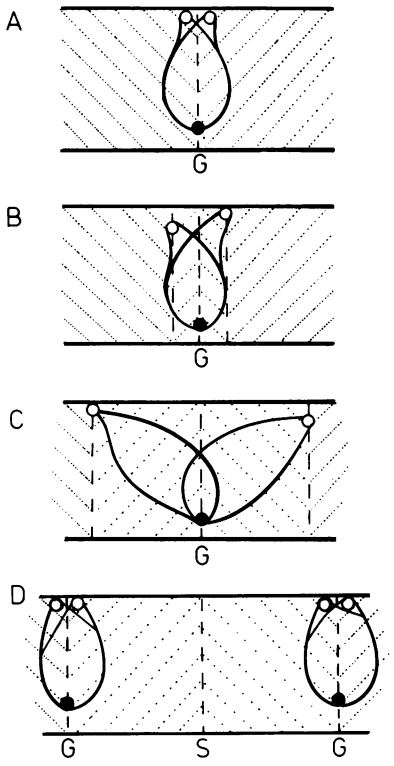

FIG. 7. *Relationship between surface growth and chromosome replication. (A–D) Stages in chromosome replication. (A) Immediately after establishment of new growth zone (G), chromosome-initiated origins (O) and terminus (●); (B) 0.2 generations after segregation (note origins moving apart but terminus at growth zone); (C) 0.8 generations after segregation; (D) Termination. Terminus detaches from growth zone and moves to junction of old and new wall formed one generation previously. Old growth zone committed to septum formation (S). Junction of oblique dotted lines represents junction of old and new cell surface.*

length extension proceeds, the origin is moved away from the bulk of the nucleus, and on completion of the chromosome the nucleus moves to the site at which the origin was attached and then attaches strongly by the terminus. There is biochemical evidence that the chromosome is more strongly attached by the terminus than by the origin (42). If nuclear segregation is achieved by a single symmetrical growth zone, then n, in the formula for model B, would have a value of 1.0 and cells at the point of nuclear division would be 2 l long. At this time, the length of surface synthesized is equal to 0.5 l on either side of the nucleus. After nuclear division, the daughter nuclei move to positions 25% from either end of the cell, and, therefore, to the junction of old and new surface formed one generation previously. The origin of the surface of such a cell on the point of division is shown in Fig. 8. If n is greater than 2 and growth zones operate symmetrically, surface growth cannot be the sole mechanism of chromosome segregation, and the site to which nuclei move would not be identifiable in this manner.

Although the average length at nuclear segregation is constant over a range of growth rates, studies of the frequency of nuclear division relative to cell length (36) indicate that nuclear division occurs over a range of cell lengths (coefficient of variation of mean length at nuclear division is about 0.14 on glucose and succinate [unpublished data]). Furthermore, length extension studies during thymine starvation, described above, indicate that cells are able to exceed the normal cell length at nuclear division. Schaecter et al. (38) showed that in several enteric bacteria the variation in cell length at division was less than the variation in generation time, and from this concluded that attainment of a certain length at division was an important element in commitment to division.

Experiments showing that growth occurs symmetrically around nuclei (32, 36) indicate that at about the time of nuclear division the old growth zone must cease length extension. Presumably this site is then committed to a developmental sequence, culminating in septum formation, which does not involve length extension. The observation that the rate of residual division during thymine starvation is not significantly affected by a nutritional shift whereas the rate of cell extension doubles can be

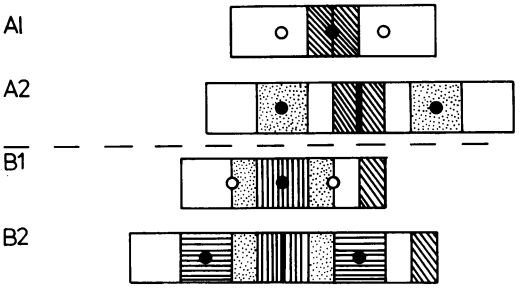

FIG. 8. *Pattern of surface growth assuming linear growth from sites of nuclear attachment. The origin of cell surface in a cell at the moment of separation is shown in B2. B1 represents this cell at the point of segregation in the same cycle. A1 and A2 represent cells at segregation and separation, respectively, in the previous cycle. Sites of nuclear attachment, ●. Sites to which nuclei move at segregation, O.*

regarded as evidence that the rate of septum formation is controlled independently of peripheral wall extension.

The dependence of the rate of linear extension on growth rate is similar to the general response of bacterial cells to a nutritional shift-up. Thus, during a shift-up, there is a rapid increase in rate of protein synthesis as a result of an increase in ribosome synthesis (15). Cell length extension is presumably dependent on membrane protein synthesis and can be expected to show the same response as cytoplasmic protein synthesis. Regulation of surface-synthesizing components must, therefore, be visualised at two levels: (i) a regulation of rate per site that is affected by the nutritional status of the growth medium; (ii) a regulation at individual sites that, when a new growth zone forms, induces formation of the necessary length-extending machinery (ribosomes for synthesis of membrane proteins, etc.).

The model for *Bacillus* growth and division, described above, has strong similarities to the model for the division of *Streptococcus faecalis* presented by Higgins et al. (9, 39). In this organism, there is evidence that (i) surface growth zones develop to become septa, i.e., septum formation occurs at a site in the newest wall; (ii) new growth zones are formed at the junction of old and new wall; (iii) growth zones operate symmetrically; (iv) there are indications that the nucleus is attached only at growth zones; (v) formation of the septum can be regarded as a developmental process to which the growth zone is committed once peripheral wall extension at that site has ceased. The essential difference between the coccal and bacillary growth forms, on this analysis, seems to be the angle at which new peripheral wall is inserted relative to old peripheral wall and the angle at which cross walls are inserted relative to the peripheral wall.

APPENDIX

Models for the determination of average cell length. The average length ($\bar{L}$) of an exponentially growing culture is given by

$$\bar{L} = \frac{\int_{a=b}^{a=1.0} L(a)\, N(a)\, da}{\int_{a=b}^{a=1.0} N(a)\, da} \quad (1)$$

where L is the cell length at relative cell age (a) and N is the cell number at cell age a given by the age distribution theorem (31) (Fig. 1b), i.e.,

$$N(a) = No\, 2^{-a} \quad (2)$$

Expressions for average length can be obtained by substituting a term for L as a function of cell age in equation 1. Linear and exponential functions have been considered.

Linear growth. Linear growth would occur during a period in which there was no change in the number of sites of length extension. Thus, in an exponentially growing culture, if the number of sites double in number at time t (a fraction of generation time), the rate of length extension doubles (Fig. 1a).

The time elapsing (in generation times) between t and cell separation equals $(m - t)$, where m is the number of cycles of cell division over which the period between t and cell separation extends. In which case, the total number of growth zones before and after t would be $n \cdot 2^{(m-1)}$ and $2 \cdot n\ 2^{(m-1)}$, respectively, i.e., during the interval $0 - t$, in a cell in which $m = 1$, the number of growth zones equals n. A cell of this kind may be regarded as one growth unit.

During the intervals of cell age a, $0 - t$, and $(t - 1.0)$, the cell length would be:

$$L = Lo + n \cdot 2^{m-1} \cdot Ka, \text{ where } o < a < t \quad (3)$$

and

$$L = Lo + [n \cdot 2^{m-1} \cdot K(t)] + [2n \cdot 2^{m-1}(a - t)K], \quad \text{where } t < a < 1.0 \quad (4)$$

where Lo is the length of a newborn cell and K is rate of length extension relative to cell age and a is relative cell age.

The length of a newborn cell is equal to the total length synthesised during one cycle, i.e.,

$$Lo = n \cdot 2^{(m-1)} \cdot K \cdot (2 - t) \quad (5)$$

Substituting equation 5 in equation 3

$$L = n \cdot 2^{(m-1)} \cdot K(a - t + 2) \quad (6)$$

and in equation 4

$$L = 2n \cdot 2^{(m-1)} \cdot K \cdot (a - t + 1) \quad (7)$$

Since L is a discontinuous function, equation 1 is solved in the form

$$\bar{L} = \frac{\int_{a=t}^{a=b} N(a)\, L(a)\, da + \int_{a=t}^{a=1} N(a)\, L(a)\, da}{\int_{a=t}^{a=1} N(a)} \quad (8)$$

substituting equations 2, 6, and 7 in equation 8

$$\bar{L} = n \cdot 2^{m-1} \cdot (K/\log_e 2) \cdot 2^{-t} \quad (9)$$

This can be expressed in real time (in contrast to relative cell age). Thus, $K = lg$, where l is the rate of length extension per site in real time and has the dimensions length per minute and $t = [(mg - x)/g]$, where x is the time (in real time) elapsing between t (in relative cell age) and cell separation. Therefore,

$$\bar{L} = (n \cdot lg)/(\log_e 2)\, 2^{x}/g \quad (10)$$

Two alternatives of this model have been considered: model A, in which l is a rate and is a constant at all growth rates (i.e., equation 10); model B, in which l is proportional to growth rate, which gives the relationship:

$$\bar{L} = (nl/\log_e 2) \cdot 2^{x}/g \quad (11)$$

in which case l has dimensions of length.

The cell length x minutes before cell separation (Lx) can be calculated as follows: Lx equals the length

of newborn cell plus length of cell synthesized between cell age 0 and $(g - x)$. In the case of model A, $Lx = 2n \cdot l \cdot g$; In the case of model B, $Lx = 2n \cdot l$. Thus, cell length at x would be a constant.

Exponential growth. Exponential growth in length would occur if: (i) new sites of length extension appeared at an exponential rate during the cell cycle, or (ii) if each site operated at an exponentially increasing rate of length extension. An expression for the time course of length extension in terms of the number of sites and rate per site can be obtained as follows. The rate of length extension per cell

$$dL/da = n(a)\, K$$

where n is the number of sites per cell at a cell age a and K is the rate of linear extension per site.

The cell length at cell age a

$$L(a) = \int n(a)\, K \cdot da$$

If the rate of length extension per site is constant (under any one growth condition) and $n(a) = n_o\, 2^a$, where n_o is the number of sites in a newborn cell

$$L(a) = (n_o\, K\, 2^a / \log_e 2) \qquad (12)$$

substituting in equation 1

$$\bar{L} = 2n_o\, K \qquad (13)$$

An expression for n_o can be obtained by postulating that at a time x minutes before cell separation the cell contains a constant number of growth zones (n) or multiples thereof. The number of growth zones at cell separation, i.e., $(2n_o) = n\ 2^{x/g}$, substituting in equation 13

$$\bar{L} = K n\, 2^{x/g} \qquad (14)$$

As with linear models, the constant K is expressed in terms of relative cell age and can be expressed in real time as lg,

$$\text{i.e., } \bar{L} = nlg2^{x/g} \qquad (15)$$

This is formally identical to model A.

If l is proportional to growth rate

$$\bar{L} = nl \cdot 2^{x/g} \qquad (16)$$

This is formally identical to model B above and has been investigated as model C above. As with model B, it can be shown that the cell length at x is a constant, i.e., from equation 12.

$$Lx = (n_o\, K / \log_e 2)\, 2^{g-x/g}$$

substituting n_o as for equation 14

$$Lx = nK/\log_e 2$$

Thus, if K is a constant, (i.e., l is proportional to growth rate), Lx is a constant at all growth rates.

Terms used.

a: Cell age (as a fraction of generation time)

g: Generation time (minutes)

K: Rate of length extension per site (micrometers per unit of cell age).

$\bar{L}$: Average cell length (micrometers)

L_o: Length of newborn cell (micrometers)

l': Constant of proportionality (micrometers per minute, model A)

l: Constant of proportionality (micrometers, model B)

m: Number of cell cycles over which time between t and cell separation extends

$N(a)$, No: Number of cells in age distribution at cell ages a and o, respectively.

Nu: Average number of nuclei per cell

n: Number of growth zones per growth unit

S: Average number of septa per cell

St: Time elapsing between appearance of septum and cell separation (minutes)

t: Time at which number of sites of length extension double in number (as a fraction of generation time)

x: Time elapsing between doubling in number of growth zones and cell separation (minutes)

y: Time elapsing between nuclear division and cell separation (minutes)

z: Time elapsing between commitment to division and cell division

ACKNOWLEDGMENTS

Valuable discussions with Howard J. Rogers and R. F. Rosenberger are gratefully acknowledged.

LITERATURE CITED

1. Chai, N. C., and K. G. Lark. 1967. Segregation of deoxyribonucleic acid in bacteria: association of the segregating unit with the cell envelope. J. Bacteriol. **94**:415-421.
2. Cole, R. M. 1965. Symposium on the fine structure and replication of bacteria and their parts. III. Bacterial cell wall replication followed by immunofluorescence. Bacteriol. Rev. **29**:326-344.
3. Collins, J. F., and M. H. Richmond. 1962. Rate of growth of *Bacillus cereus* between divisions. J. Gen. Microbiol. **28**:15-33.
4. Dix, D. E., and C. E. Helmstetter. 1973. Coupling between chromosome completion and cell division in *Escherichia coli*. J. Bacteriol. **115**:786-795.
5. Donachie, W. D., and K. J. Begg. 1970. Growth of the bacterial cell. Nature (London) **227**:1220-1225.
6. Donachie, W. D., D. T. M. Martin, and K. J. Begg. 1971. Independence of cell division and DNA replication in *Bacillus subtilis*. Nature (London) New Biol. **231**:274-276.
7. Eberle, H., and K. G. Lark. 1966. Chromosome segregation in *Bacillus subtilis*. J. Mol. Biol. **22**:183-186.
8. Helmstetter, C. E., S. Cooper, O. Pierucci, and E. Revelos. 1968. On the bacterial life sequence. Cold Spring Harbor Symp. Quant. Biol. **33**:809-822.
9. Higgins, M. L., and G. D. Shockman. 1970. Model for cell wall growth in *Streptococcus faecalis*. J. Bacteriol. **101**:643-648.
10. Hoffman, B., W. Messer, and U. Schwarz. 1972. Regulation of polar cap formation in the life cycle of *Escherichia coli*. J. Supramol. Struct. **1**:29-37.
11. Hughes, R. C., and E. Stokes. 1971. Cell wall growth in *Bacillus licheniformis* followed by immunofluorescence with mucopeptic specific antiserum. J. Bacteriol. **106**:694-696.
12. Jacob, F., S. Brenner, and F. Cuzin. 1963. On the regulation of DNA replication in bacteria. Cold Spring Harbor Symp. Quant. Biol. **28**:329-347.
13. James, T. W. 1960. Controlled division synchrony and

growth in Protozoan micro-organisms. Ann. N.Y. Acad. Sci. **90**:550–564.
14. Kepes, A., and F. Autissier. 1972. Topology of membrane growth in bacteria. Biochim. Biophys. Acta **265**:443–469.
15. Kjeldgaard, N. O., O. Maaløe, and M. Schaecter. 1958. The transition between different physiological states during balanced growth of *S. typhimurium*. J. Gen. Microbiol. **19**:607–616.
16. Koch, A. L. 1970. Turbidity measurements of bacterial cultures in some commercial instruments. Anal. Biochem. **38**:252–259.
17. Kubitschek, H. E. 1970. Evidence for the generality of linear cell growth. J. Theoret. Biol. **28**:15–29.
18. Kubitschek, H. E. 1971. Control of cell growth in bacteria experiments with thymine starvation. J. Bacteriol. **105**:472–476.
19. Kubitschek, H. E., M. L. Freedman, and S. Silver. 1971. Potassium uptake in synchronous and synchronised cultures of *Escherichia coli*. Biophys. J. **11**:787–797.
20. Lapidus, J. R. 1971. Analysis of a model for multiseptation in bacteria. J. Bacteriol. **108**:607–608.
21. Lark, K. G., H. Eberle, R. A. Consigli, H. C. Minorko, N. Chai, and C. Lark. 1967. Chromosome segregation and the regulation of DNA replication, p. 63–89. *In* H. J. Vogel, J. O. Lampen, and V. Bryson (ed.), Organizational biosynthesis. Academic Press Inc., New York.
22. Marr, A. G., R. J. Harvey, and W. C. Trentini. 1966. Growth and division of *Escherichia coli*. J. Bacteriol. **91**:2388–2389.
23. Mauck, J., L. Chan, and L. Glaser. 1972. Model of cell wall growth of *Bacillus megaterium*. J. Bacteriol. **109**:373–378.
24. Mindich, L., and S. Dales. 1972. Membrane synthesis in *Bacillus subtilis*. III. Morphological localisation of sites of membrane synthesis. J. Cell Biol. **55**:32–41.
25. Morrison, D. C., and H. J. Morowitz. 1970. Studies on membrane synthesis in *Bacillus megaterium*, K. M. J. Mol. Biol. **49**:441–459.
26. Ohki, M. 1972. Correlation between metabolism of phosphatidyl glycerol and membrane synthesis in *Escherichia coli*. J. Mol. Biol. **68**:249–264.
27. Paulton, R. J. L. 1970. Analysis of the multiseptate potential of *Bacillus subtilis*. J. Bacteriol. **104**:762–767.
28. Pierucci, O., and C. Zuchowski. 1973. Non-random segregation of DNA strands in *Escherichia coli* B/r. J. Mol. Biol. **80**:477–503.
29. Previc, E. P. 1970. Biochemical determination of bacterial morpology and the geometry of cell division. J. Theoret. Biol. **27**:471–497.
30. Pritchard, R. H. 1974. On the growth and form of a bacterial cell. Philos. Trans. R. Soc. London **267**:303–336.
31. Powell, E. O. 1956. Growth rate and generation time of bacteria with special reference to continuous culture. J. Gen. Microbiol. **15**:492–511.
32. Ryter, A. 1971. Etude de la croissance de la membrane chez *Bacillus subtilis* au moyen de la distribution des flagelles. Ann. Inst. Pasteur Paris. **121**:271–288.
33. Ryter, A., Y. Hirota, and U. Schwarz. 1973. Process of cellular division in *Escherichia coli*. Growth pattern of *Escherichia coli* murein. J. Mol. Biol. **78**:185–195.
34. Sargent, M. G. 1973. Synchronous cultures of *Bacillus subtilis* obtained by filtration with glass fiber filters. J. Bacteriol. **116**:736–740.
35. Sargent, M. G. 1973. Membrane synthesis in synchronous cultures of *Bacillus subtilis* 168. J. Bacteriol. **116**:397–409.
36. Sargent, M. G. (1974). Nuclear segregation in *Bacillus subtilis*. Nature (London). **250**:252–254.
37. Schaecter, M., O. Maaløe, and N. O. Kjeldgaard. 1958. Dependency on medium and temperature of cell size and chemical composition during balanced growth of *S. typhimurium*. J. Gen. Microbiol. **19**:592–606.
38. Schaecter, M., J. P. Williamson, J. R. Wood, and A. L. Koch. 1962. Growth, cell and nuclear divisions in some bacteria. J. Gen. Microbiol. **29**:421–434.
39. Shockman, G. D., L. Daneo-Moore, and M. L. Higgins. 1974. Problems of cell wall and membrane growth, enlargment and division. Ann. N.Y. Acad. Sci. **235**:161–197.
40. Sud, I. J., and M. Schaecter. 1964. Dependence on the content of cell envelope on the growth rate of *Bacillus megaterium*. J. Bacteriol. **88**:1612–1617.
41. Ward, C. B., and D. A. Glaser. 1971. Correlation between rate of cell growth and rate of DNA synthesis in *Escherichia coli* B/r. Proc. Natl. Acad. Sci. U.S.A. **68**:1061–1064.
42. Yamaguchi, K., and H. Yoshikawa. 1973. Topography of chromosome membrane function in *Bacillus subtilis*. Nature (London) New Biol. **244**:204–206.
43. Zaritsky, A., and R. H. Pritchard. 1973. Changes in cell size and shape associated with changes in the replication time of the chromosome of *Escherichia coli*. J. Bacteriol. **114**:824–837.